Systemic Translocation of *S. aureus* Drives Anti-CD4 Autoimmunity in Treated HIV Infection

Short title: Autoimmunity in HIV immunopathogenesis

Da Cheng[1], Zhenwu Luo[1], Wangbin Ning[1], Sonya L. Heath[2], Magnus Gisslen[3,4,5], Richard W Price[6], Ruth Adekunle[7,8], Tabinda Salman[1], Douglas Johnson[1], John E McKinnon[7,8], Lishomwa C. Ndhlovu[9], Wenhui Hu[10], Wei Jiang[1,7,8*] (ORCiD 0000-0002-1374-053X)

[1]Department of Pharmacology and Immunology, Medical University of South Carolina, Charleston, SC, 29425, USA.

[2]Division of Infectious Diseases, Department of Medicine, University of Alabama at Birmingham, Birmingham, AL, 35294, USA.

[3]Department of Infectious Diseases, Institute of Biomedicine, Sahlgrenska Academy, University of Gothenburg, 41645, Gothenburg, Sweden

[4]Department of Infectious Diseases, Sahlgrenska University Hospital, Region Västra Götaland,Gothenburg, Sweden

[5]Public Health Agency of Sweden, Solna, Sweden

[6]Department of Neurology, University of California, San Francisco, San Francisco General Hospital, San Francisco, CA, 94110, USA

[7]Department of Medicine, Division of Infectious Diseases, Medical University of South Carolina, Charleston, SC, 29425, USA.

[8]Ralph H. Johnson VA Medical Center, Charleston, SC, USA

[9]Department of Medicine, Division of Infectious Diseases, Weill Cornell Medicine, New York, NY, 10021, USA

[10]Department of Anatomy and Neurobiology, Virginia Commonwealth University, Richmond, Virginia, 23298-0709, USA

*Corresponding author: Wei Jiang, 173 Ashley Ave. Charleston, SC, 29425, email: jianw@musc.edu

Abstract

Background: Anti-CD4 autoantibodies in people with HIV (PWH) receiving suppressive antiretroviral therapy (ART) appear to prevent CD4+ T cell reconstitution, yet the mechanisms underlying their production remain unclear. Emerging evidence implicates *Staphylococcus aureus* and its peptidoglycan (PGN) in autoimmunity.

Methods: Plasma from 32 ART-naive PWH, 53 ART-treated PWH, and 32 HIV-negative controls was analyzed for IgG autoantibodies and markers of *S. aureus* translocation. Causality was examined in EcoHIV-infected mice administered PGN from *S. aureus* or *Bacillus subtilis*. PGN structure was analyzed via mass spectrometry.

Results: Among 87 autoantibodies, 40% were elevated in ART-naive PWH and largely normalized by ART; however, anti-CD4 IgGs remained elevated in PWH on ART. Anti-CD4 IgG levels inversely correlated with CD4+ T cell counts in ART-treated PWH and positively with *S. aureus* translocation. In mice, *S. aureus* PGN induced anti-CD4 IgGs, reduced gut CD4+ T cells, and promoted surface IgG binding and apoptosis in CD4+ T cells.

Conclusion: *S. aureus* and its PGN translocation may contribute to anti-CD4 autoimmunity and hinder immune recovery in ART-treated PWH, representing a potential therapeutic target.

Keywords: HIV, autoimmunity, anti-CD4 autoantibodies, *Staphylococcus aureus* PGN, failed immune reconstitution, microbiome

Introduction

Recent studies from us and others reveal that autoimmunity contributes to pathogenesis in infectious diseases without clinical autoimmune diseases (Bastard *et al*, 2020; Koning *et al*, 2021; Manry *et al*, 2022; Ning *et al*, 2022b). Approximately 20% of people with HIV (PWH) on antiretroviral therapy (ART) fail to restore CD4+ T cell counts despite plasma viral suppression, leading to increased risks of comorbidities and mortality (Gazzola *et al*, 2009). We demonstrate that anti-CD4 autoantibodies mediate CD4+ T cell death via antibody-mediated cytotoxicity (ADCC) and contributes to poor immune reconstitution following ART (Luo *et al*, 2017a). The effects of anti-CD4 IgG on CD4+ T cell depletion in HIV were further reported by Lisco et al. (Lisco *et al*, 2019). However, the mechanism driving anti-CD4 IgG production during HIV infection remains unknown.

Our previous study revealed that *Staphylococcus aureus* PGN promoted pathogenic autoantibody production and kidney damage in systemic lupus erythematosus (SLE) (Ning *et al*, 2022a). Intraperitoneal (i.p.) injection of heat-killed *S. aureus* or its peptidoglycan (PGN) induced pathogenic autoantibody production in C57BL/6J and autoimmune-prone mice (Luo *et al*, 2019; Ning *et al.*, 2022a). PGN is a major component of the bacterial cell wall and is highly antigenic. PGNs from different bacteria can lead to different immune regulatory activities (Wolf & Underhill, 2018). *S. aureus* nasal colonization is more common in PWH (Rossetti *et al*, 2019). Thus, we

investigated the role of *S. aureus* or its PGN in anti-CD4 IgG production and found that *S. aureus* translocation contributes to anti-CD4 IgG production and poor immune recovery in PWH from ART.

Results

HIV-associated IgG autoantibody landscape and the unique characteristics of anti-CD4 IgG

We assessed 87 autoantibody IgGs (autoIgGs) from healthy controls, untreated PWH (HIV+/ART-naive), and PWH on suppressive ART (HIV+/ART+). Levels of 35 autoIgGs (40%) were increased and 3 autoIgGs were decreased in HIV+/ART+ compared to controls, while the rest showed similar levels (Figure 1A). ART was associated with normalized autoIgGs except for anti-CD4 and anti-prothrombin protein IgGs, which remained elevated in PWH on ART (HIV+/ART+, Figures 1A-1B). Anti-CD8 IgG levels were unexpectedly lower in HIV+/ART-naive versus controls (Figure 1C). Notably, an inverse correlation was observed between plasma anti-CD4 IgG levels and CD4+ T cell counts in HIV+/ART+ but not in the other two groups (Figure 1D). Moreover, anti-CD4 IgM and IgA levels were similar across the groups. Among anti-CD4 IgGs, IgG1 and IgG3, but not IgG2 or IgG4, were elevated in HIV+/ART+ compared to controls, linking them to persistent low CD4+ T cell counts and poor recovery after ART (Figure S1A-S1B) (Luo *et al.*, 2017a; Song *et al*, 2020).

Elevated anti-CD4 IgG levels are associated with serologic and cellular markers of *S. aureus* translocation in PWH on suppressive ART

Next, we found that plasma levels of IgGs against *S. aureus* antigens were positively correlated with plasma anti-CD4 IgGs in the HIV+/ART+ group (Figure 2A-2B). In the

B-cell RNA sequencing analysis, the *S. aureus* signaling pathway differed between the HIV+/high versus HIV+/low anti-CD4 IgG groups as well as the HIV+/high anti-CD4 IgG group versus controls (Figure 2C).

Administration of *S. aureus* PGN led to anti-CD4 IgG production in EcoHIV mice

We established and confirmed EcoHIV infection in the mouse model and virus dose titration (Figure S2). In the current study, serum levels of anti-CD4 IgG, but not total IgG, were increased in the *S. aureus* PGN group compared to controls (Figure 3A-3B), indicating that *S. aureus* PGN-mediated antibody production has limited polyclonal B cell activation. The main subtypes of anti-CD4 IgG increased in HIV+/ART+ were IgG1 and IgG3, supporting its ADCC activity (de Taeye *et al*, 2020; Rozsnyay *et al*, 1989). In mice, IgG2a and IgG2b, but not IgG1, mediate ADCC activity (Kipps *et al*, 1985). Notably, anti-CD4 IgG2b and IgG3 were increased among *S. aureus* PGN-elevated subclasses (Figure 3C).

Administration of *S. aureus* PGN decreased the percentages of gut CD4+ T cells likely indirectly via increased highly apoptotic IgG binding CD4+ T cells in EcoHIV mice

To investigate whether *S. aureus* PGN induces pathogenic anti-CD4 IgGs that mediate CD4+ T cell death *in vivo*, we evaluated the percentage of CD4+ T cells in the gut, blood, and spleen. Notably, the percentages of CD3+CD4+ T cells among total CD3+

T cells decreased (Figure 3D-3E), and the frequencies of autoreactive IgG surface binding on CD4+ T cells increased (Figure 4A-4B) in mesenteric lymph nodes and not in the blood or spleens of *S. aureus* PGN-treated mice compared to the control. In all three sites tested, IgG+CD4+ T cells were highly apoptotic, but not IgG–CD4+ T cells (Figure 4C). However, in contrast to gut CD4+CD3+ T cells, *S. aureus* PGN did not decrease the percentage of gut CD4−CD3+ T cells among total CD3+ T cells; also, we found that gut CD4−CD3+ T cells rarely had surface autoIgG binding (Figure S3). Moreover, *S. aureus* PGN did not directly induce gut CD4+ T cell apoptosis *in vitro* (Figure S4). These results indicate that *S. aureus* PGN may induce gut CD4+ T cell apoptosis indirectly through autoIgG binding to the CD4+ T cell surface.

S. aureus PGN drove CSR via TLR2

As indicated in Figure 3C, serum anti-CD4 IgG2b and IgG3 subclasses increased in response to *S. aureus* PGN. CSR is a crucial biological process for antibody maturation in response to both foreign antigens and self-antigens in the germinal center (Mietzner *et al*, 2008). Here, *S. aureus* PGN, but not *B. subtilis* PGN, promoted CSR to IgG2b and IgG3 via TLR2 *in vitro* (Figure 5A-5B; Figure S6) in response to the optimal PGN concentration (Figure S5A-S5B). Notably, after denaturing any contaminating proteins, heat-inactivated *S. aureus* PGN exhibited similar CSR induction compared with the untreated PGN (Figure S5C). Furthermore, *B. subtilis* PGN induced greater TLR2

signaling activity compared to *S. aureus* PGN (Figure S5D), suggesting that *S. aureus* PGN-mediated CSR did not exclusively account for its ability to activate TLR2.

PGN structural analysis of *S. aureus* and *B. subtilis*

The length of the sugar polymers of PGN varies among bacterial species; *S. aureus* consists of ~18 disaccharides, while *Bacillus* has 80-250 disaccharides (Wolf & Underhill, 2018). In this study, *S. aureus* PGN exhibited the total hydrolysate containing muramic acid (Mur) and the amino acids lysine (Lys), alanine (Ala), glycine (Gly) and glutamic acid (Glu). Quantification of amino acids by GC/MS of N-heptafluorobutyric amino acid isobutylesters shows the molar ratio: 1.4 Ala: 2.9 Gly: 1.0 Glu: 1.1 Lys. *B. subtilis* PGN exhibited the total hydrolysate containing Mur and the amino acids diaminopimelic acid (Dpm), Ala, and Glu. The molar ratio is 1.0 Ala: 1.0 Glu: 0.8 Dpm. The analysis of enantiomers of the total hydrolysate showed the presence of meso-Dpm and DGlu. In summary, *S. aureus* PGN was A3α (L-Lys-Gly5-6) L-Lys -Gly3 whereas *B. subtilis* PGN was A1γ meso-Dpm-direct, providing the foundation of their differences in immunomodulatory activities.

Discussion

Autoimmunity plays a pathogenic role in infectious diseases in the absence of any clinical autoimmune disease (Bastard *et al.*, 2020; Koning *et al.*, 2021; Manry *et al.*, 2022). During HIV infection, CD4+ T cell depletion characterizes immune non-responders as their CD8+ T cell counts are increased compared to healthy controls (Luo *et al.*, 2017a). Despite extensive research on poor CD4+ T cell recovery post ART, no study has proposed a CD4-specific mechanism (Zhang *et al*, 2021) until we first reported anti-CD4 IgG autoimmunity in HIV (Luo *et al.*, 2017a). The effects of anti-CD4 IgG on CD4+ T cell depletion in HIV were further reported by other colleagues (Ouyang *et al*, 2025) (Lisco *et al.*, 2019). Here, we reveal that anti-CD4 IgG autoimmunity is driven by a specific microbiome *S. aureus*. Notably, PWH from Africa show a higher failure rate of CD4+ T cell recovery following suppressive ART (Lawn *et al*, 2006) as well as a higher rate of *S. aureus* infection or colonization; thus, there may be a causal link between *S. aureus* translocation, anti-CD4 IgG autoimmunity, and immune reconstitution failure in HIV (Olalekan *et al*, 2012).

Although anti-CD4 IgG was studied in the pre-ART era, its pathogenic activity was not proven (Chams *et al*, 1991; Sekigawa *et al*, 1991) until 2017 when we reported evidence of anti-CD4 IgG-mediated CD4+ T cell death and poor immune recovery following ART (Luo *et al.*, 2017a). Recently, a study revealed that plasma anti-CD4 IgG levels increased during HIV infection prior to ART initiation and decreased after ART,

however, levels remained higher in some PWH on ART (Song *et al.*, 2020). Moreover, an inverse association between plasma anti-CD4 IgG levels and CD4+ T cell counts after 48 and 96 weeks of ART, but not during pre-ART or after 24 weeks of ART were reported (Song *et al.*, 2020). Low-affinity nonfunctional or natural autoantibodies can be induced under persistent inflammation (Hunziker *et al*, 2003). The development of a pathogenic autoantibody may occur over many years due to disordered somatic hypermutation and CSR (Elkon & Casali, 2008). Indeed, we reveal that anti-CD4 IgGs from PWH on ART but not from ART-naive induce ADCC (Cheng *et al*, 2023). Thus, differing from HIV+/ART+, anti-CD4 IgGs from untreated PWH are likely natural autoantibodies without cytotoxicity and are generated by high viremia and cytokine storms. Autoimmune features in HIV often develop after ART initiation (Iordache *et al*, 2014; Zandman-Goddard & Shoenfeld, 2002). These results imply that pathogenic autoantibodies develop post-ART.

S. aureus colonization and antigen translocation may not be sufficient to induce pathogenic autoantibody production unless a compromised barrier, host immune perturbations, or a genetic background susceptible to autoimmunity. Differing from autoantibodies in autoimmune diseases, pathogenic anti-CD4 IgG in PWH on suppressive ART may result from the following factors: 1) remaining higher rates of apoptotic CD4+ T cells lead to increased CD4 self-antigen, especially in the lymph nodes (Luo *et al*, 2017b); 2) viral proteins are constantly released despite suppressive

ART (Folkvord *et al*, 2005; Heesters *et al*, 2015; Ramratnam *et al*, 2004; Rothenberger *et al*, 2015); HIV gp120 increases the binding of CD4 to anti-CD4 antibodies of PWH (Sekigawa *et al.*, 1991). Consequently, HIV gp120-CD4 accumulates in lymph nodes and promotes anti-CD4 IgG production (Lederman *et al*, 2011); 3) most PWH do not have the genetic background of autoimmune diseases.

Although CD4+ T cell apoptosis was observed only in the mesenteric lymph nodes and not in the spleen after 3-month administration of *S. aureus* PGN, evidence is known that SIV/HIV infection leads to CD4+ T cell depletion starting from the gut during acute infection, and develops to peripheral CD4+ T cell depletion during chronic infection due to exhaustion (Veazey, 2019). We hypothesize that long-term (e.g., one year) administration of *S. aureus* PGN may eventually deplete peripheral CD4+ T cells. Notably, *S. aureus* PGN increased the frequencies of autoIgG binding to the surface of CD4+ T cells in the gut but not in the spleen and blood; the IgG+CD4+ T cells were highly apoptotic. Mesenteric CD4+ T cell death was not induced by *S. aureus* PGN directly *in vitro*. These findings suggest that *S. aureus* PGN may induce mesenteric CD4+ T cell apoptosis indirectly through autoIgG binding on CD4+ T cells and subsequently exert an ADCC effect. Nonetheless, the mechanisms of *S. aureus* PGN-mediated gut autoIgG production related to CD4+ T cell decline deserve further investigation.

The main limitation is the potential contamination in the *S. aureus* PGN preparation we purchased, which could contain other components (e.g., *Staphylococcal* protein A, surface protein A, and lipoteichoic acid [LTA]). However, strong evidence supports the role of *S. aureus* PGN in autoantibody production, as follows: 1) a TLR2 inhibitor blocked the PGN effects; 2) PGNs can be detected in the circulation in healthy humans without clinical infections (Huang *et al*, 2019; Molinaro *et al*, 2019; Wolf & Underhill, 2018); 3) only non-protein bacterial antigens can be detected in the blood in humans (Azzouz *et al*, 2019; Brenchley *et al*, 2006); 4) heat inactivation did not reduce CSR; 5) Staph Protein A and *Staphylococcus* Enterotoxin B reduced SLE severity in lupus-prone mice (Braun *et al*, 2000; Kim *et al*, 1991); 6) *S. aureus* LTA predominately induced pro-inflammatory cytokines in myeloid cells, but failed to induce autoantibodies (Danforth *et al*, 1995; Ning *et al.*, 2022a; Skinner *et al*, 2005; Standiford *et al*, 1994). In this translational study, we revealed fundamental findings *in vivo* through autoantibody screening using human samples and verified causality using an HIV mouse model.

In summary, this is the first study to show the role of *S. aureus* translocation in inducing pathogenic anti-CD4 IgGs and CD4+ T cell depletion in HIV, which may provide novel therapies targeting *S. aureus* colonization or translocation (e.g., receptor inhibitors and probiotics), and help improve CD4+ T cell recovery and reduce morbidity in PWH on suppressive ART.

Materials and methods

Human subjects

This study included 32 uninfected controls, 32 untreated PWH (HIV+/ART-naive), and 53 PWH on ART (HIV+/ART+, $\geq$ 2 years of undetectable plasma HIV-1 RNA). All participants were recruited from the Sahlgrenska University Hospital, San Francisco General Hospital, and the Medical University of South Carolina (MUSC) (Gisslen *et al*, 2021; Jiang *et al*, 2021). This study was approved by the local institutional review board. The clinical information is shown in Table 1. PWH were stratified into low and high anti-CD4 IgG subgroups based on a cutoff of 35 ng/ml, determined from 95th percentile in healthy controls.

Autoantigen protein array, B-cell gene profiles, and plasma levels of anti-CD4 IgG and subclasses, IgM, and IgA

In recent studies, we described the methods of protein array containing 87 self-antigens, microarray for B-cell gene expression profiles, and plasma anti-CD4 autoantibody levels (Luo *et al.*, 2019; Luo *et al.*, 2017a).

Plasma *S. aureus* antigen translocation

S. aureus lysate was prepared using the BugBuster Master Mix and coated onto plates at 2 µg/100 µL/well at 4°C overnight. The plate was blocked with PBS containing 3% BSA. Diluted plasma samples (1:4000 for IgA, 1:400000 for IgG) were added and

incubated under RT for 60 minutes. Detection was performed using horseradish peroxidase-labeled anti-human IgG and IgA via 405 nm absorbance with ABTS.

Bacterial PGN structural analysis using mass spectrometry

PGNs from *S. aureus* (ATCC, 6538P) and *B. subtilis* (NR-607, BEI, Manassas, VA) were separated with an Agilent HPLC system and analyzed using mass spectrometry (Creative Proteomics, Shirley, NY, USA).

Animal Experiments

Six-week-old female C57BL/6J mice (Jackson Laboratory, Bar Harbor, ME) were housed at a specific pathogen-free (SPF) facility at MUSC. EcoHIV plasmid (GFP labeled) was obtained from Dr. Hu from Virginia Commonwealth University (Yin *et al*, 2016; Yin *et al*, 2017). Briefly, we administered mixed antibiotics (Gibco™ Antibiotic Mixture) in the drinking water (1mg/mL) for 3 days, and stopped for 2 days. Next, EcoHIV virus was i.p. injected into B6 mice (50 μL of virus 3.45 x 10^8 IU/mL, n=6 per group) once. Two weeks post-infection, the mice were i.p. injected with PBS, *S. aureus,* or *B. subtilis* PGN (InvivoGen, San Diego, CA) twice per week for 12 weeks.

Mouse serum anti-CD4 IgG levels

The 96-well plate was coated with 1 μg/100 μL/well of recombinant mouse CD4 protein (Sino Biological, Wayne, PA) at 4°C overnight. After blocking with 3% BSA, diluted

serum samples were added and horseradish peroxidase-labeled anti-mouse IgG or its subclasses were used. Absorbance was measured at 405 nm with ASBT.

B cell class switch DNA recombination (CSR)

B cells were isolated from the spleen of 8-week-old unmanipulated mice using the B Cell Negative Isolation Kit (STEMCELL, Vancouver, BC). B cells were cultured with medium or SA-PGN or BS-PGN (10 μg/mL), +/- anti-TLR2 neutralizing antibody or isotype IgG2a (InvivoGen, 100 ng/mL), or a positive control (LPS from *Escherichia coli* 055:B5 [3 μg/mL, InvivoGen] plus IFN-γ [50 ng/mL, BioLegend] or TGF-β1 [2 ng/mL, R&D Systems, Minneapolis, MN]). CSR was analyzed by the percentages of proliferating IgG3 and IgG2b cells using a BD FACSVerse™ Cell Analyzer (BD, San Jose, CA) after surface staining with anti-B220 (RA3-6B2), anti-IgG2b (RMG2b-1), anti-IgG3 (R40-82), anti-CD138 (281-2), and anti-IgM (RMM-1) from BioLegend.

IgG surface binding on CD4+ T cells

At the end of the study, cells from blood, spleens, and mesenteric lymph nodes were collected, stained with anti-CD3 (17A2), anti-CD4 (GK1.5), anti-IgG (Poly4053, BioLegend), Annexin V (BD Pharmingen), anti-B220 (RA3-6B2), anti-CD19 (1D3), anti-F4/80 (BM8), anti-IgM (RMM-1), and streptavidin (1:1000, BD Pharmingen), and analyzed using a BD FACSVerse™ flow cytometer and FlowJo software.

PGN-mediated TLR2 activity

TLR2 activity was detected using the HEK-Blue™ mTLR2 cells (InvivoGen) following the manufacturer's instruction.

Statistics

Data were analyzed using Student's t-test or Mann-Whitney test for comparisons between two groups, and one-way ANOVA with the Kruskal-Wallis test for comparisons involving more than two groups. Associations were evaluated using Spearman's correlation test. $P < 0.05$ was considered statistically significant.

Authors' contributions

D.C. wrote the first version of the manuscript. D.C., Z.L., T.S., D.J., and W.N. performed experiments and analyzed data. M.G., R.W., S.H., and Z.L. recruited the study participants. D.C., Z.L., W.J., L.N., R.P., W. H., M.G., JEM, and R.A. were involved in critically revising the manuscript.

Conflicts of Interest

The authors declare no competing interests.

Acknowledgments

We would like to thank John D. Dinolfo, Ph.D. from MUSC for English Language editing. This work was supported by Ralph H. Johnson VA Medical Center, Merit Review Award Number (CX002422, Jiang) from the United States (U.S.) Department of Veterans Affairs (VA) Office of Research and Development (CSR&D) Service, the VA Southeast Network 7 Research Development Award (RDA, Adekunle), the National Institute on Drug of Abuse (R01DA059854, Jiang), National Institute of Allergy and Infectious Diseases (P30AI027767, Saag/Health), National Institute of Health (R01NS094067, Price), the Swedish state, under an agreement between the Swedish government and the county councils (ALF agreement ALFGBG-965885), and the National Center for Advancing Translational Sciences of the National Institutes of Health under Award Number UL1TR001450 (the pilot grant, Jiang), TL1TR002382 (Adekunle), and UL1TR002378 (TL1 grant, Adekunle). The content is solely the responsibility of the authors and does not necessarily represent the official views of the National Institutes of Health.

Availability of data and materials

Microarray data are available in GEO (Gene Expression Omnibus, https://www.ncbi.nlm.nih.gov/geo/query/acc.cgi?acc=GSE109837) under accession number GSE109837.

Figure legends

Figure 1. **HIV-associated IgG autoantibodies.** (A) Z-scored plasma levels of 87 autoantibodies in controls (n = 32), untreated PWH (n = 32), and ART-suppressed PWH (n = 53). (B) Anti-CD4 and anti-prothrombin IgG levels. (C) Anti-CD8 IgG levels. (D) Correlation between anti-CD4 IgG levels and CD4+ T cell counts. ANOVA and Spearman correlation tests were applied.

Figure 2. Association of *S. aureus* serological and cellular markers with anti-CD4 IgG in PWH on ART. (A) Positive correlation between plasma anti-CD4 IgG and anti-*S. aureus* IgG levels. (B) Subgroup of HIV+/ART+ individuals shows elevated anti-*S. aureus* IgG. (C–D) B cell gene expression analysis reveals enriched immune pathways in PWH vs. controls. Spearman correlation and ANOVA were applied; $P < 0.05$.

Figure 3. *S. aureus* PGN induces anti-CD4 IgG and reduces gut CD4+ T Cells in EcoHIV mice. C57BL/6J mice received i.p. injections of PBS, *S. aureus* PGN, or *B. subtilis* PGN twice weekly for 12 weeks (n = 8/group). (A–C) Serum levels of anti-CD4 IgG, total IgG, and anti-CD4 IgG subclasses. (D–E) Gating strategy and CD4+ T cell percentages in mesenteric lymph nodes, spleen, and blood. Student's t-test and ANOVA were applied. *, P < 0.05; **, P < 0.01; ***, P < 0.001; ****, P < 0.0001.

Figure 4. *S. aureus* PGN increases apoptotic IgG+CD4+ T Cells in gut-Associated tissues in EcoHIV mice. (A) Annexin V binding on IgG+CD4+ vs. IgG–CD4+ T cells. (B–D) Frequencies of IgG+CD4+ T cells in mesenteric lymph nodes, spleen, and

blood. (E–G) Annexin V binding on IgG+CD4+ and IgG−CD4+ T cells in the same tissues. Student's t-test and one-way ANOVA were applied.

Figure 5. ***S. aureus* PGN induced CSR to IgG2b and IgG3 *in vitro***. Splenic B cells from unmanipulated C57BL/6J mice werecultured with the medium (control), *S. aureus* (SA) or *B. subtilis* (BS) PGN (10 μg/mL) plus TLR2-mAb or isotype Ab (1μg/mL) for 96 hours. The percentages of proliferating IgG2b+ and IgG3+ B cells (%CFSE^{low}IgG2b/IgG3+ in IgG2b/Ig3+B220+ cells) (A-B) are shown. ANOVA tests.

Figure S1. **Elevated plasma levels of anti-CD4 IgG1 and IgG3 subclasses in PWH on ART**. (A) The median plasma levels of anti-CD4 IgG, IgM, and IgA were evaluated in healthy controls (n = 15) and HIV+/ART+ subjects (n = 23). (B) The median plasma levels of anti-CD4 IgG subclasses (IgG1-IgG4) were determined in controls and HIV+/ART+ subjects. Mann-Whitney tests.

Figure S2. Confirmation of established EcoHIV infection in the mouse model. EcoHIV virus was i.p. injected into B6 mice with EcoHIV and verified using qPCR in blood samples.

Figure S3. ***S. aureus* PGN did not decrease the percent of gut CD4−CD3+ T cells in total CD3+ T cells, and rare cells from gut CD4−CD3+ T cells had surface IgG**

binding. (A) Gating strategies and (B) percentages of CD4−CD3+ T cells in total CD3+ T cells and IgG+CD4−CD3+ T cells in the mesenteric lymph nodes. ANOVA tests.

Figure S4. ***S. aureus* PGN did not induce mesenteric CD4+ T cell apoptosis directly *in vitro*.** Lymphocytes from mesenteric lymph nodes were treated with *S. aureus* PGN (0.1-10 μg/mL) for 4 days. (A) Annexin V binding on the surface of CD4+ T cells, percentages of CD4+ T cells (B) and annexin V binding on CD4+ T cells were calculated. ANOVA tests.

Figure S5. **Dose titration of PGN for CSR and TLR2 activity**. Different doses of *S. aureus* PGN (0.1-10 μg/mL) for the induction of the percentages of total IgG2b+ B cells (A) and proliferating IgG2b+ B cells (B). (C) Comparison of CSR induction by heat-inactivated vs. untreated *S. aureus* PGN. (D) mTLR2 reporter cell line was treated with PBS and different doses of *S. aureus* PGN or *B. subtilis* PGN (0.1-10 μg/mL) for 16 hours. The mTLR2 activation was determined using a spectrophotometer at 620 nm. ANOVA tests.

Figure S6. *S. aureus* PGN induced CSR to IgG2b and IgG3 in plasmablast cells *in vitro*. Splenic B cells from unmanipulated mice were cultured with *S. aureus* (SA), or *B. subtilis* (BS) PGN (10 μg/mL) for 96 hours.Percentages of IgG2b+ and IgG3+

plasmablast cells (%CD138+CFSE^{low}IgG2b/IgG3+ in B220+ cells) (A-B) are shown. ANOVA tests.

Table 1 Clinical characteristics of study subjects

	HIV-negative (n = 32)	HIV+/ART naive (n = 32)	HIV+/ART+ (n = 53)	P value (two HIV+ groups)
Age (years)	49 (34-58)	49 (35-55)	42 (36-52)	0.16
Sex ratio, male: female	21:11	22:10	37:16	0.92
CD4+ T cell counts	797 (554-916)	255 (98-490)	570 (456-724)	< 0.0001
Nadir CD4+ T cell counts		215 (97-490)	294 (164-464)	0.37
Duration of ART (years)			5.5 (4-6)	

ART, antiretroviral therapy; CD4+ T cell count (cells/µL)

Data are means (25th percentile, 75th percentile)

References

Azzouz D, Omarbekova A, Heguy A, Schwudke D, Gisch N, Rovin BH, Caricchio R, Buyon JP, Alekseyenko AV, Silverman GJ (2019) Lupus nephritis is linked to disease-activity associated expansions and immunity to a gut commensal. *Ann Rheum Dis* 78: 947-956

Bastard P, Rosen LB, Zhang Q, Michailidis E, Hoffmann HH, Zhang Y, Dorgham K, Philippot Q, Rosain J, Beziat V *et al* (2020) Autoantibodies against type I IFNs in patients with life-threatening COVID-19. *Science* 370

Braun N, Erley C, Klein R, Kotter I, Saal J, Risler T (2000) Immunoadsorption onto protein A induces remission in severe systemic lupus erythematosus. *Nephrol Dial Transplant* 15: 1367-1372

Brenchley JM, Price DA, Schacker TW, Asher TE, Silvestri G, Rao S, Kazzaz Z, Bornstein E, Lambotte O, Altmann D *et al* (2006) Microbial translocation is a cause of systemic immune activation in chronic HIV infection. *Nat Med* 12: 1365-1371

Chams V, Idziorek T, Klatzmann D (1991) Biological properties of anti-CD4 autoantibodies purified from HIV-infected patients. *AIDS* 5: 565-569

Cheng D, Luo Z, Fitting S, Stoops W, Heath SL, Ndhlovu LC, Jiang W (2023) The link between chronic cocaine use, B cell perturbations, and blunted immune recovery in HIV-infected individuals on suppressive ART. *NeuroImmune Pharm Ther* 2: 71-79

Danforth JM, Strieter RM, Kunkel SL, Arenberg DA, VanOtteren GM, Standiford TJ (1995) Macrophage inflammatory protein-1 alpha expression in vivo and in vitro: the role of lipoteichoic acid. *Clin Immunol Immunopathol* 74: 77-83

de Taeye SW, Bentlage AEH, Mebius MM, Meesters JI, Lissenberg-Thunnissen S, Falck D, Senard T, Salehi N, Wuhrer M, Schuurman J *et al* (2020) FcgammaR Binding and ADCC Activity of Human IgG Allotypes. *Frontiers in immunology* 11: 740

Elkon K, Casali P (2008) Nature and functions of autoantibodies. *Nat Clin Pract Rheumatol* 4: 491-498

Folkvord JM, Armon C, Connick E (2005) Lymphoid follicles are sites of heightened human immunodeficiency virus type 1 (HIV-1) replication and reduced antiretroviral effector mechanisms. *AIDS Res Hum Retroviruses* 21: 363-370

Gazzola L, Tincati C, Bellistri GM, Monforte A, Marchetti G (2009) The absence of CD4+ T cell count recovery despite receipt of virologically suppressive highly active antiretroviral therapy: clinical risk, immunological gaps, and therapeutic options. *Clin Infect Dis* 48: 328-337

Gisslen M, Keating SM, Spudich S, Arechiga V, Stephenson S, Zetterberg H, Di Germanio C, Blennow K, Fuchs D, Hagberg L *et al* (2021) Compartmentalization of cerebrospinal fluid inflammation across the spectrum of untreated HIV-1 infection, central nervous system injury and viral suppression. *PLoS One* 16: e0250987

Heesters BA, Lindqvist M, Vagefi PA, Scully EP, Schildberg FA, Altfeld M, Walker BD, Kaufmann DE, Carroll MC (2015) Follicular Dendritic Cells Retain Infectious HIV in Cycling Endosomes. *PLoS Pathog* 11: e1005285

533 Huang Z, Wang J, Xu X, Wang H, Qiao Y, Chu WC, Xu S, Chai L, Cottier F, Pavelka
534 N *et al* (2019) Antibody neutralization of microbiota-derived circulating peptidoglycan
535 dampens inflammation and ameliorates autoimmunity. *Nat Microbiol* 4: 766-773
536 Hunziker L, Recher M, Macpherson AJ, Ciurea A, Freigang S, Hengartner H,
537 Zinkernagel RM (2003) Hypergammaglobulinemia and autoantibody induction
538 mechanisms in viral infections. *Nat Immunol* 4: 343-349
539 Iordache L, Launay O, Bouchaud O, Jeantils V, Goujard C, Boue F, Cacoub P,
540 Hanslik T, Mahr A, Lambotte O *et al* (2014) Autoimmune diseases in HIV-infected
541 patients: 52 cases and literature review. *Autoimmun Rev* 13: 850-857
542 Jiang W, Luo Z, Stephenson S, Li H, Di Germanio C, Norris PJ, Fuchs D, Zetterberg
543 H, Gisslen M, Price RW (2021) Cerebrospinal Fluid and Plasma Lipopolysaccharide
544 Levels in Human Immunodeficiency Virus Type 1 Infection and Associations With
545 Inflammation, Blood-Brain Barrier Permeability, and Neuronal Injury. *J Infect Dis* 223:
546 1612-1620
547 Kim C, Siminovitch KA, Ochi A (1991) Reduction of lupus nephritis in MRL/lpr mice
548 by a bacterial superantigen treatment. *J Exp Med* 174: 1431-1437
549 Kipps TJ, Parham P, Punt J, Herzenberg LA (1985) Importance of immunoglobulin
550 isotype in human antibody-dependent, cell-mediated cytotoxicity directed by murine
551 monoclonal antibodies. *J Exp Med* 161: 1-17
552 Koning R, Bastard P, Casanova JL, Brouwer MC, van de Beek D, with the
553 Amsterdam UMCC-BI (2021) Autoantibodies against type I interferons are associated
554 with multi-organ failure in COVID-19 patients. *Intensive Care Med* 47: 704-706
555 Lawn SD, Myer L, Bekker LG, Wood R (2006) CD4 cell count recovery among HIV-
556 infected patients with very advanced immunodeficiency commencing antiretroviral
557 treatment in sub-Saharan Africa. *BMC Infect Dis* 6: 59
558 Lederman MM, Calabrese L, Funderburg NT, Clagett B, Medvik K, Bonilla H,
559 Gripshover B, Salata RA, Taege A, Lisgaris M *et al* (2011) Immunologic failure
560 despite suppressive antiretroviral therapy is related to activation and turnover of
561 memory CD4 cells. *The Journal of infectious diseases* 204: 1217-1226
562 Lisco A, Wong CS, Lage SL, Levy I, Brophy J, Lennox J, Manion M, Anderson MV,
563 Mejia Y, Grivas C *et al* (2019) Identification of rare HIV-1-infected patients with
564 extreme CD4+ T cell decline despite ART-mediated viral suppression. *JCI Insight* 4
565 Luo Z, Li M, Wu Y, Meng Z, Martin L, Zhang L, Ogunrinde E, Zhou Z, Qin S, Wan Z *et*
566 *al* (2019) Systemic translocation of Staphylococcus drives autoantibody production in
567 HIV disease. *Microbiome* 7: 25
568 Luo Z, Li Z, Martin L, Wan Z, Meissner EG, Espinosa E, Wu H, Yu X, Fu P, Julia
569 Westerink MA *et al* (2017a) Pathological Role of Anti-CD4 Antibodies in HIV-Infected
570 Immunologic Nonresponders Receiving Virus-Suppressive Antiretroviral Therapy. *J*
571 *Infect Dis* 216: 82-91
572 Luo Z, Zhou Z, Ogunrinde E, Zhang T, Li Z, Martin L, Wan Z, Wu H, Qin Z, Ou T *et al*
573 (2017b) The effect of plasma auto-IgGs on CD4+ T cell apoptosis and recovery in
574 HIV-infected patients under antiretroviral therapy. *J Leukoc Biol*

Manry J, Bastard P, Gervais A, Le Voyer T, Rosain J, Philippot Q, Michailidis E, Hoffmann HH, Eto S, Garcia-Prat M *et al* (2022) The risk of COVID-19 death is much greater and age dependent with type I IFN autoantibodies. *Proc Natl Acad Sci U S A* 119: e2200413119

Mietzner B, Tsuiji M, Scheid J, Velinzon K, Tiller T, Abraham K, Gonzalez JB, Pascual V, Stichweh D, Wardemann H, Nussenzweig MC (2008) Autoreactive IgG memory antibodies in patients with systemic lupus erythematosus arise from nonreactive and polyreactive precursors. *Proc Natl Acad Sci U S A* 105: 9727-9732

Molinaro R, Mukherjee T, Flick R, Philpott DJ, Girardin SE (2019) Trace levels of peptidoglycan in serum underlie the NOD-dependent cytokine response to endoplasmic reticulum stress. *J Biol Chem* 294: 9007-9015

Ning W, Cheng D, Howe PH, Bian C, Kamen DL, Luo Z, Fu X, Ogunrinde E, Yang L, Wang X *et al* (2022a) Staphylococcus aureus peptidoglycan (PGN) induces pathogenic autoantibody production via autoreactive B cell receptor clonal selection, implications in systemic lupus erythematosus. *J Autoimmun* 131: 102860

Ning W, Xu W, Cong X, Fan H, Gilkeson G, Wu X, Hughes H, Jiang W (2022b) COVID-19 mRNA vaccine BNT162b2 induces autoantibodies against type I interferons in a healthy woman. *J Autoimmun* 132: 102896

Olalekan AO, Schaumburg F, Nurjadi D, Dike AE, Ojurongbe O, Kolawole DO, Kun JF, Zanger P (2012) Clonal expansion accounts for an excess of antimicrobial resistance in Staphylococcus aureus colonising HIV-positive individuals in Lagos, Nigeria. *Int J Antimicrob Agents* 40: 268-272

Ouyang Y, Wu K, Fu L, Yi P, Cheng D, Fu X (2025) Effect of anti-CD4 mAb induced by inhibiting B cell disorder on immune reconstruction of HIV-infected immunological non-responders. *Mol Med* 31: 244

Ramratnam B, Ribeiro R, He T, Chung C, Simon V, Vanderhoeven J, Hurley A, Zhang L, Perelson AS, Ho DD, Markowitz M (2004) Intensification of antiretroviral therapy accelerates the decay of the HIV-1 latent reservoir and decreases, but does not eliminate, ongoing virus replication. *J Acquir Immune Defic Syndr* 35: 33-37

Rossetti B, Lombardi F, Belmonti S, D'Andrea MM, Tordini G, D'Avino A, Borghetti A, Moschese D, De Luca A, Montagnani F (2019) Nasopharingeal bacterial and fungal colonization in HIV-positive versus HIV-negative adults. *New Microbiol* 42: 37-42

Rothenberger MK, Keele BF, Wietgrefe SW, Fletcher CV, Beilman GJ, Chipman JG, Khoruts A, Estes JD, Anderson J, Callisto SP *et al* (2015) Large number of rebounding/founder HIV variants emerge from multifocal infection in lymphatic tissues after treatment interruption. *Proc Natl Acad Sci U S A* 112: E1126-1134

Rozsnyay Z, Sarmay G, Walker M, Maslanka K, Valasek Z, Jefferis R, Gergely J (1989) Distinctive role of IgG1 and IgG3 isotypes in Fc gamma R-mediated functions. *Immunology* 66: 491-498

Sekigawa I, Groopmen JE, Allan JD, Ikeuchi K, Biberfield G, Takatsuki K, Byrn RA (1991) Characterization of autoantibodies to the CD4 molecule in human immunodeficiency virus infection. *Clinical immunology and immunopathology* 58:

145-153
Skinner NA, MacIsaac CM, Hamilton JA, Visvanathan K (2005) Regulation of Toll-like receptor (TLR)2 and TLR4 on CD14dimCD16+ monocytes in response to sepsis-related antigens. *Clin Exp Immunol* 141: 270-278
Song A, Li Z, Luo Z, Lu X, Wang R, Liu L, Xia W, Wan Z, Zhang T, Su B *et al* (2020) Effects of Early and Delayed Antiretroviral Therapy on Plasma Anti-CD4 Autoreactive IgG and Its Association With CD4(+) T-Cell Recovery in Acute HIV-Infected Individuals. *Front Pharmacol* 11: 449
Standiford TJ, Arenberg DA, Danforth JM, Kunkel SL, VanOtteren GM, Strieter RM (1994) Lipoteichoic acid induces secretion of interleukin-8 from human blood monocytes: a cellular and molecular analysis. *Infect Immun* 62: 119-125
Veazey RS (2019) Intestinal CD4 Depletion in HIV / SIV Infection. *Curr Immunol Rev* 15: 76-91
Wolf AJ, Underhill DM (2018) Peptidoglycan recognition by the innate immune system. *Nat Rev Immunol* 18: 243-254
Yin C, Zhang T, Li F, Yang F, Putatunda R, Young WB, Khalili K, Hu W, Zhang Y (2016) Functional screening of guide RNAs targeting the regulatory and structural HIV-1 viral genome for a cure of AIDS. *AIDS* 30: 1163-1174
Yin C, Zhang T, Qu X, Zhang Y, Putatunda R, Xiao X, Li F, Xiao W, Zhao H, Dai S *et al* (2017) In Vivo Excision of HIV-1 Provirus by saCas9 and Multiplex Single-Guide RNAs in Animal Models. *Mol Ther* 25: 1168-1186
Zandman-Goddard G, Shoenfeld Y (2002) HIV and autoimmunity. *Autoimmun Rev* 1: 329-337
Zhang Y, Jiang T, Li A, Li Z, Hou J, Gao M, Huang X, Su B, Wu H, Zhang T, Jiang W (2021) Adjunct Therapy for CD4(+) T-Cell Recovery, Inflammation and Immune Activation in People Living With HIV: A Systematic Review and Meta-Analysis. *Front Immunol* 12: 632119

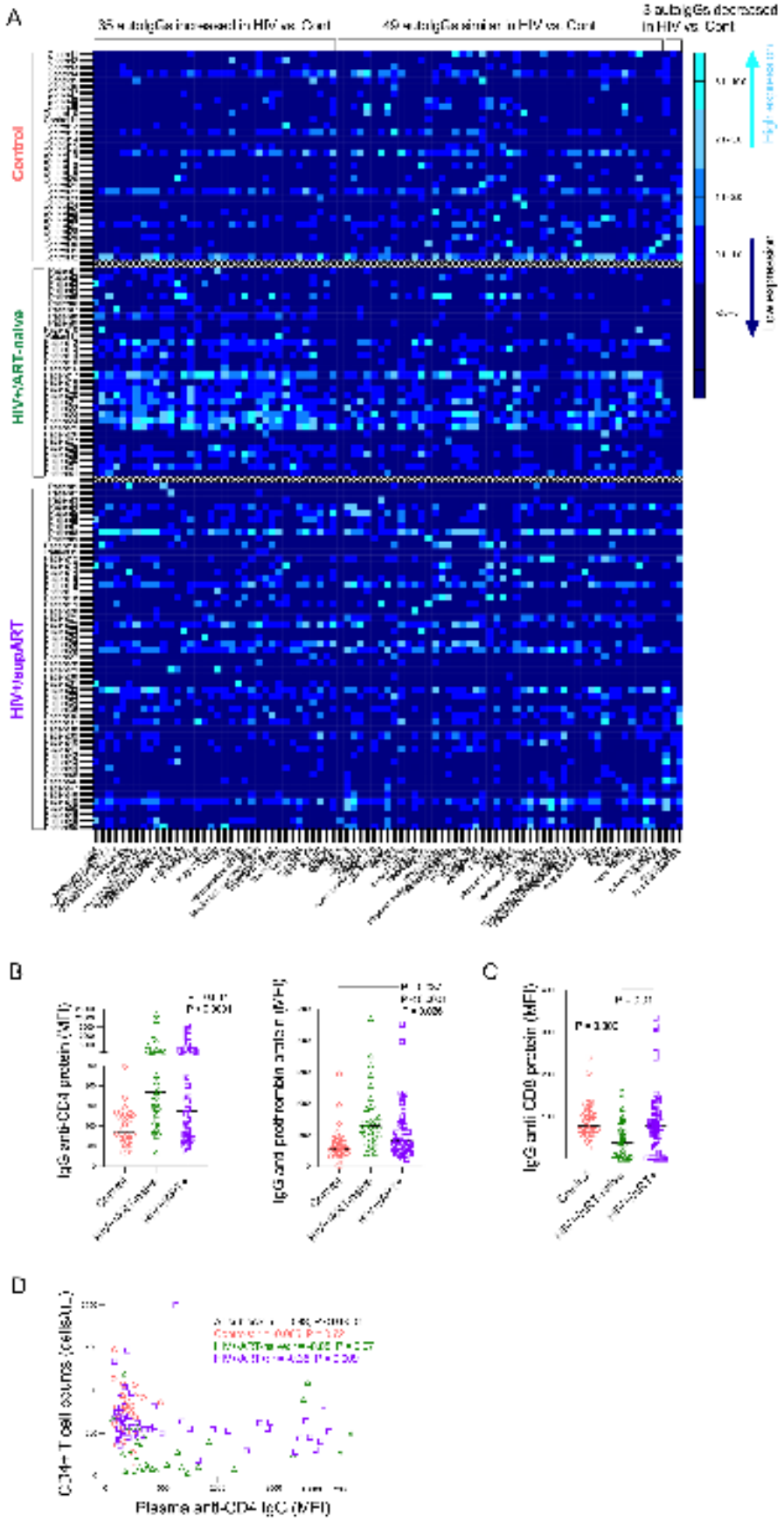
A
Control
HIV+/ART-naïve
HIV+/suppART
B
C
D
Plasma anti-CD4 IgG (MFI)

Figure 1

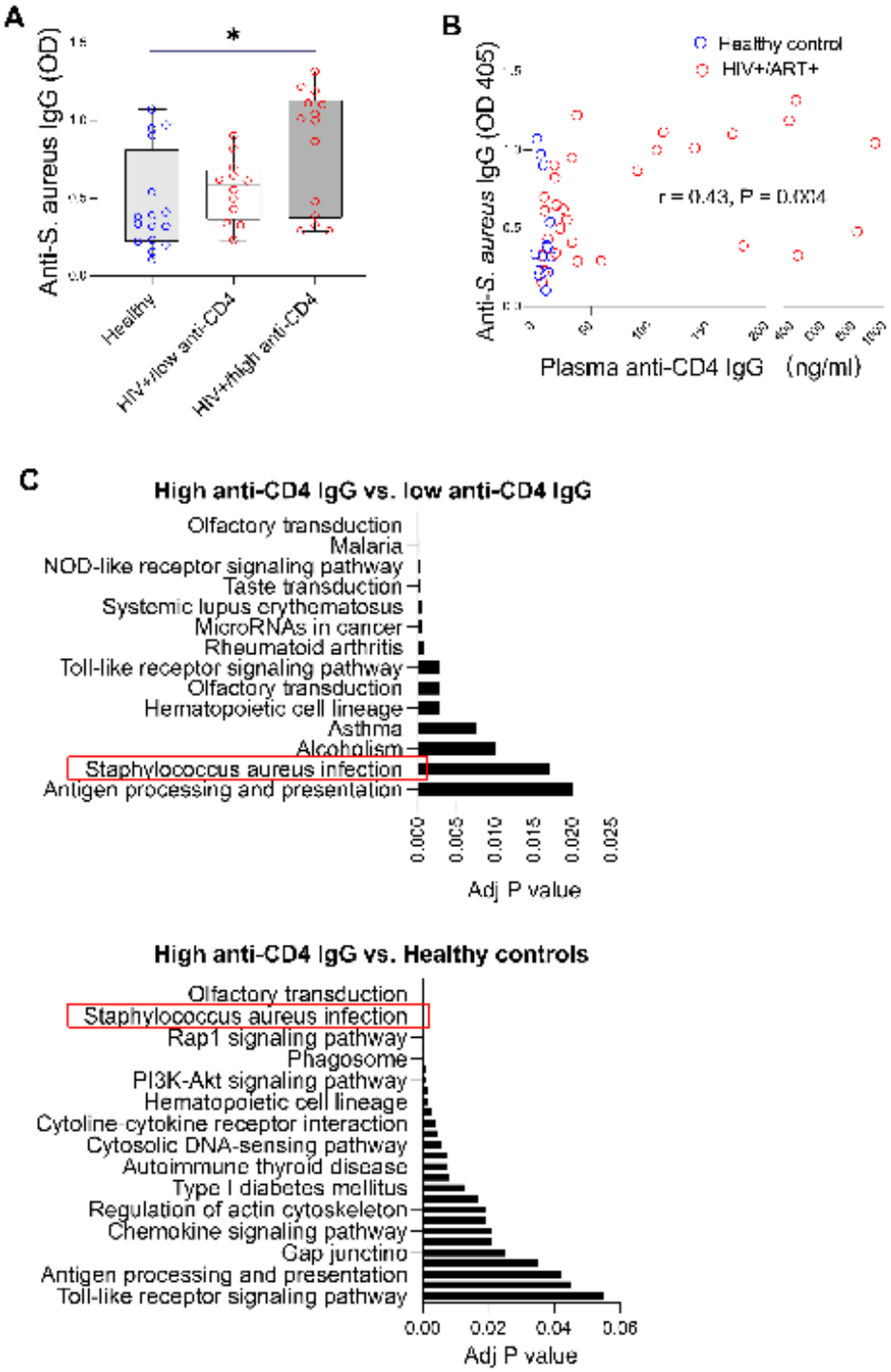
A
Anti-S. aureus IgG (OD)
*
Healthy
HIV+/low anti-CD4
HIV+/high anti-CD4
B
Healthy control
HIV+/ART+
Anti-S. aureus IgG (OD 405)
r = 0.43, P = 0.004
Plasma anti-CD4 IgG (ng/ml)
C
High anti-CD4 IgG vs. low anti-CD4 IgG
Olfactory transduction
Malaria
NOD-like receptor signaling pathway
Taste transduction
Systemic lupus erythematosus
MicroRNAs in cancer
Rheumatoid arthritis
Toll-like receptor signaling pathway
Olfactory transduction
Hematopoietic cell lineage
Asthma
Alcoholism
Staphylococcus aureus infection
Antigen processing and presentation
0.000
0.005
0.010
0.015
0.020
0.025
Adj P value
High anti-CD4 IgG vs. Healthy controls
Olfactory transduction
Staphylococcus aureus infection
Rap1 signaling pathway
Phagosome
PI3K-Akt signaling pathway
Hematopoietic cell lineage
Cytoline-cytokine receptor interaction
Cytosolic DNA-sensing pathway
Autoimmune thyroid disease
Type I diabetes mellitus
Regulation of actin cytoskeleton
Chemokine signaling pathway
Gap junction
Antigen processing and presentation
Toll-like receptor signaling pathway
0.00
0.02
0.04
0.06
Adj P value

Figure 2

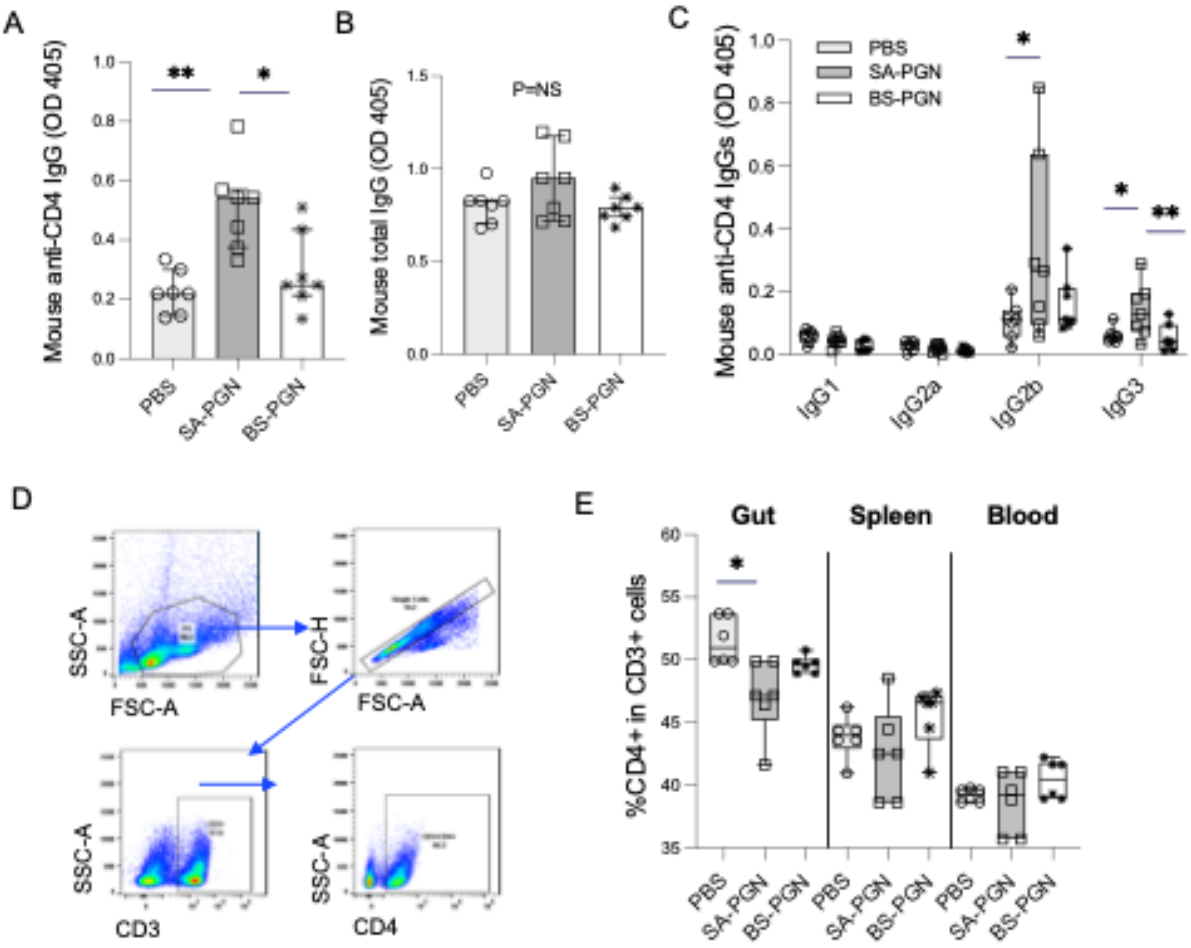
A
Mouse anti-CD4 IgG (OD 405)
PBS
SA-PGN
BS-PGN
B
Mouse total IgG (OD 405)
P=NS
C
Mouse anti-CD4 IgGs (OD 405)
IgG1
IgG2a
IgG2b
IgG3
D
SSC-A
FSC-A
FSC-H
CD3
CD4
E
Gut
Spleen
Blood
%CD4+ in CD3+ cells

Figure 3

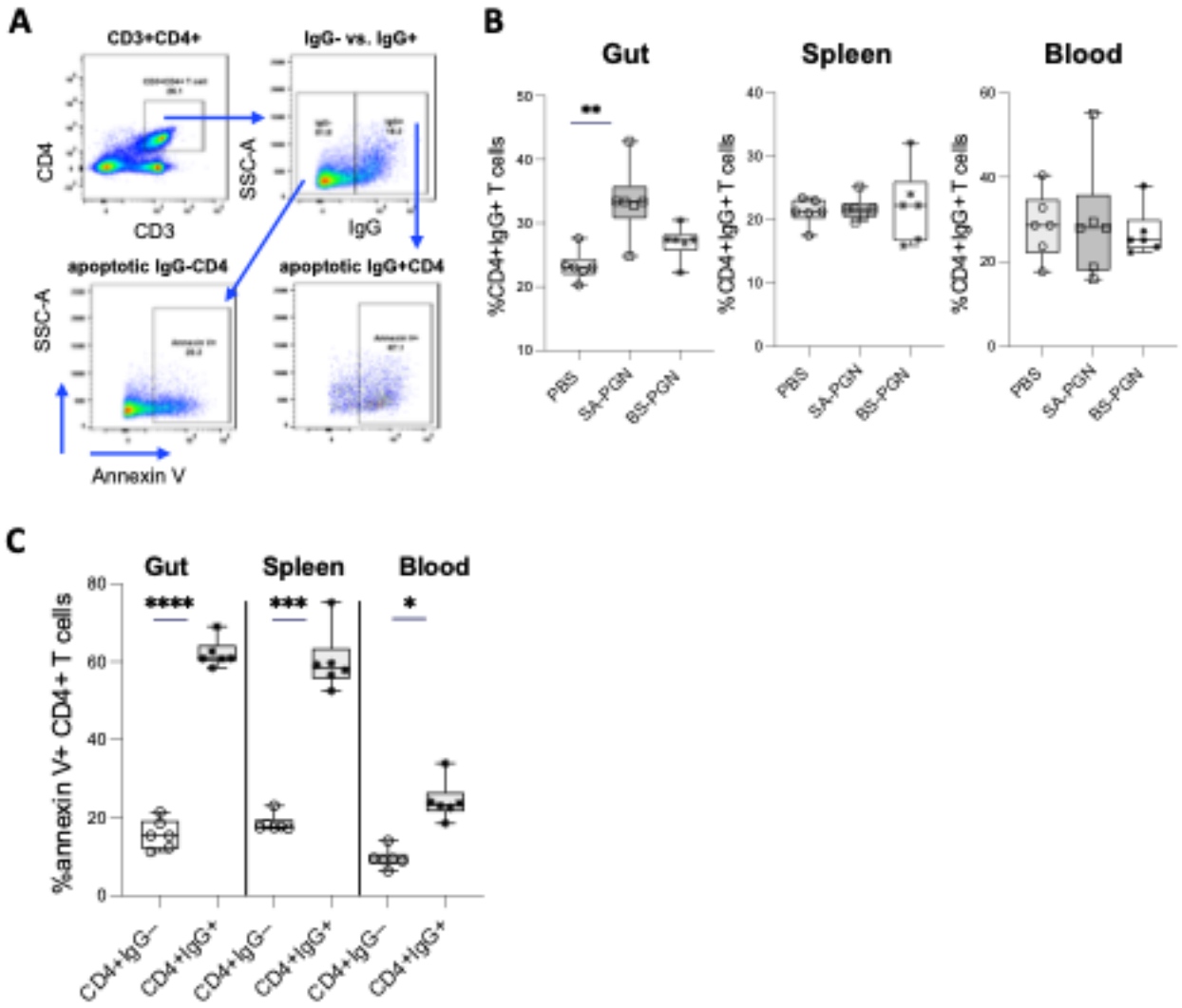
A
CD3+CD4+
IgG- vs. IgG+
CD4
CD3
SSC-A
IgG
apoptotic IgG-CD4
apoptotic IgG+CD4
SSC-A
Annexin V
B
Gut
Spleen
Blood
%CD4+IgG+ T cells
**
PBS
SA-PGN
BS-PGN
C
Gut
Spleen
Blood
%annexin V+ CD4+ T cells
****
***
*
CD4+IgG−
CD4+IgG+

Figure 4

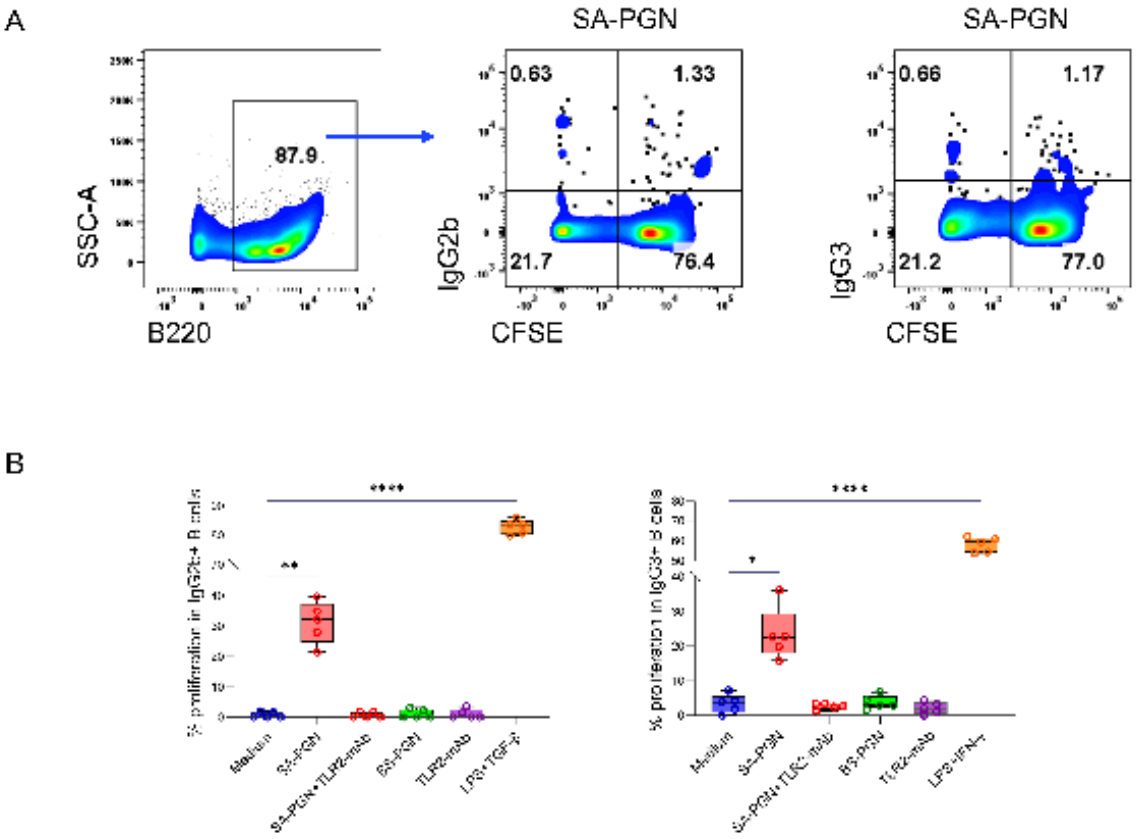
A
SA-PGN
SA-PGN
87.9
SSC-A
B220
0.63
1.33
21.7
76.4
IgG2b
CFSE
0.66
1.17
21.2
77.0
IgG3
CFSE
B
Medium
SA-PGN
SA-PGN+TLR2-mAb
BS-PGN
TLR2-mAb
LPS+TGF-β
Medium
SA-PGN
SA-PGN+TLR2-mAb
BS-PGN
TLR2-mAb
LPS+IFN-γ

Figure 5

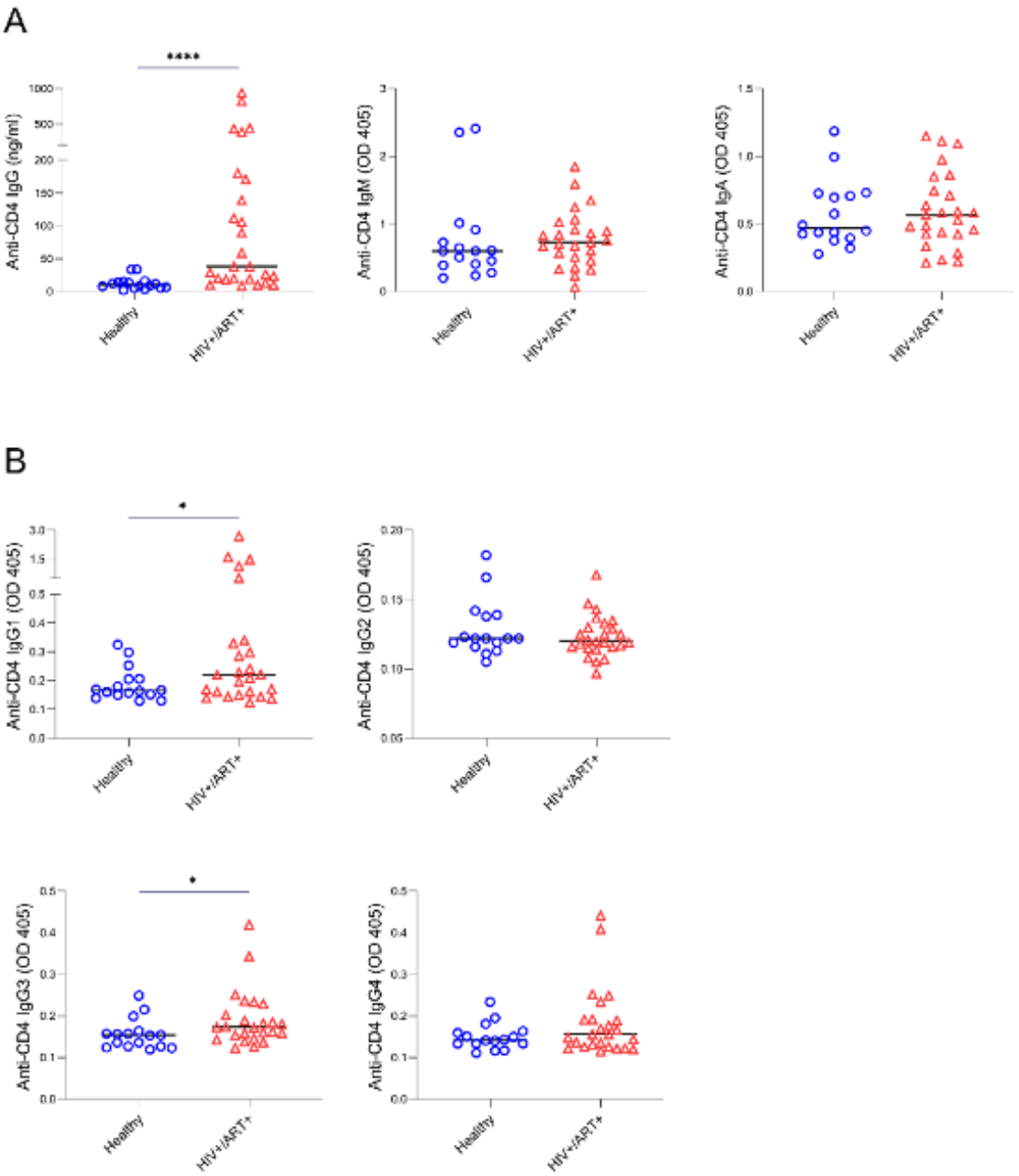

Figure S1

674

675

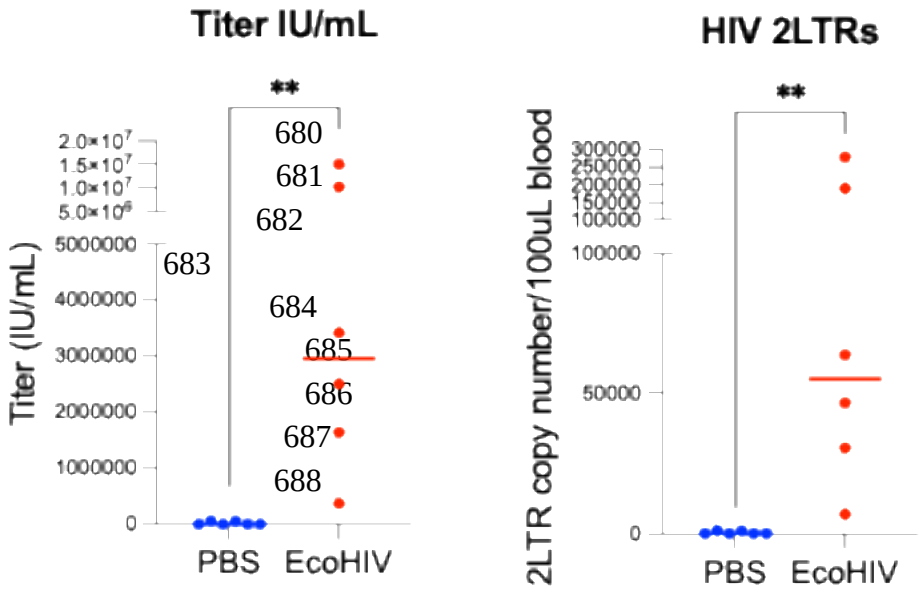
Titer IU/mL
**
Titer (IU/mL)
2.0×10^7
1.5×10^7
1.0×10^7
5.0×10^6
5000000
4000000
3000000
2000000
1000000
0
PBS
EcoHIV
HIV 2LTRs
**
2LTR copy number/100uL blood
300000
250000
200000
150000
100000
100000
50000
0
PBS
EcoHIV

Figure S2

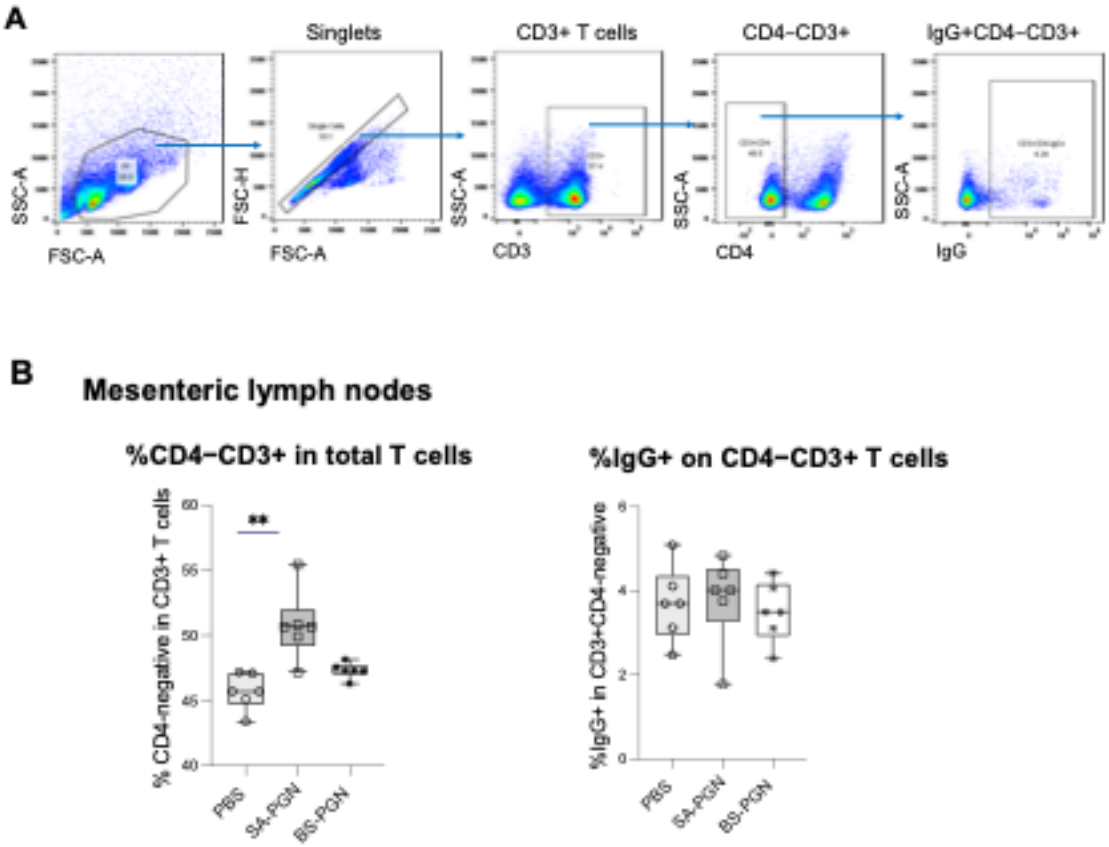
A
Singlets
CD3+ T cells
CD4−CD3+
IgG+CD4−CD3+
SSC-A
FSC-A
FSC-H
FSC-A
SSC-A
CD3
SSC-A
CD4
SSC-A
IgG
B
Mesenteric lymph nodes
%CD4−CD3+ in total T cells
% CD4-negative in CD3+ T cells
**
PBS
SA-PGN
BS-PGN
%IgG+ on CD4−CD3+ T cells
%IgG+ in CD3+CD4-negative
PBS
SA-PGN
BS-PGN

Figure S3

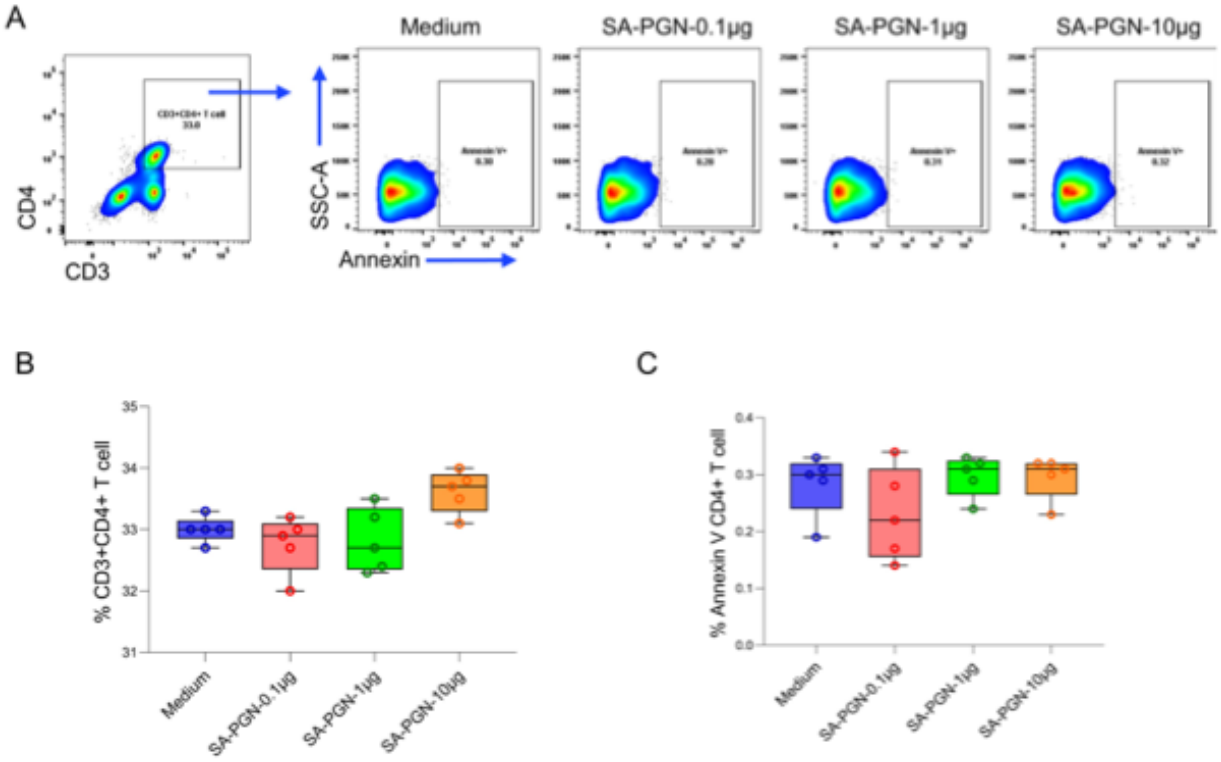

Figure S4

708

709

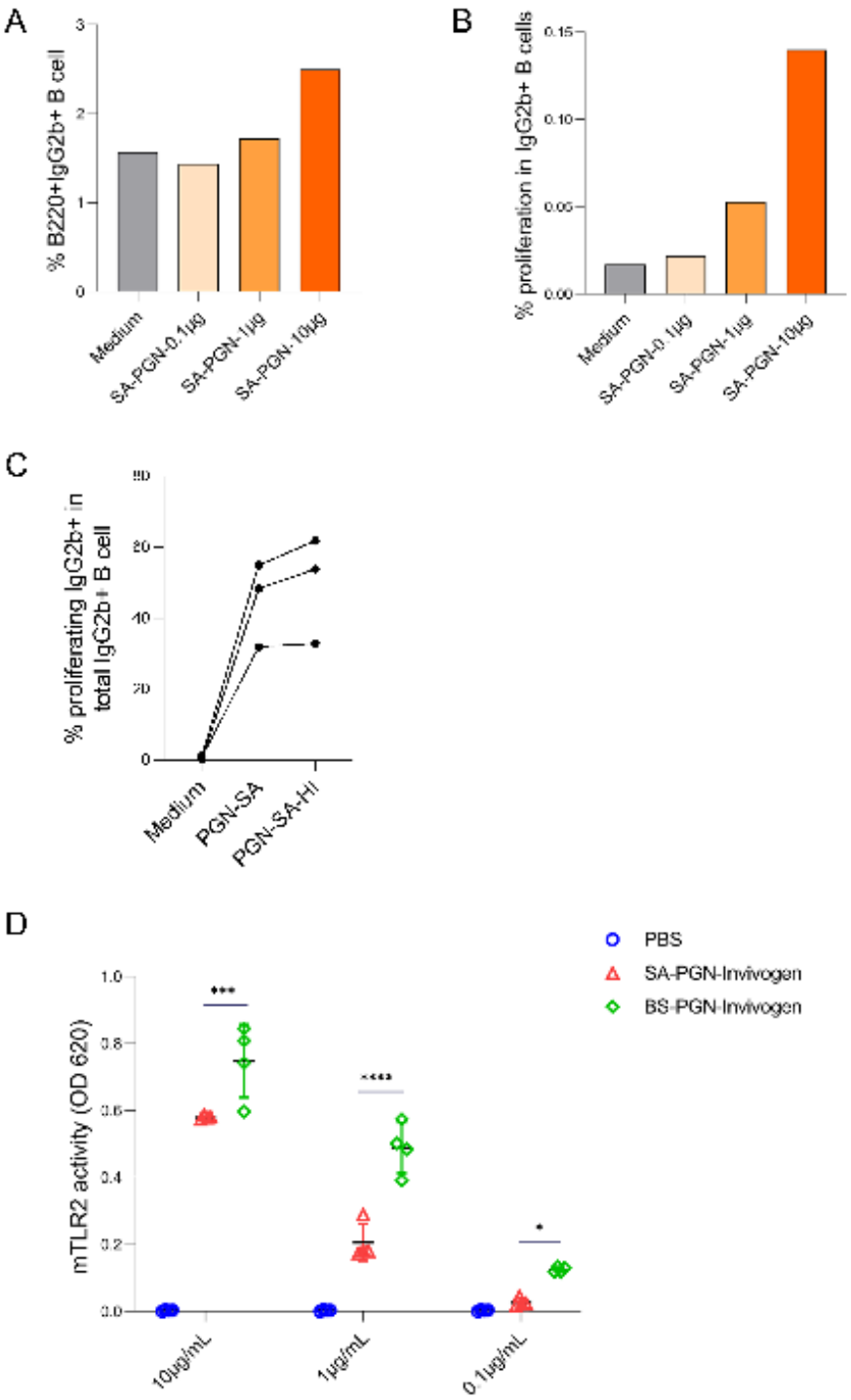
A
% B220+IgG2b+ B cell
Medium
SA-PGN-0.1µg
SA-PGN-1µg
SA-PGN-10µg
B
% proliferation in IgG2b+ B cells
Medium
SA-PGN-0.1µg
SA-PGN-1µg
SA-PGN-10µg
C
% proliferating IgG2b+ in total IgG2b+ B cell
Medium
PGN-SA
PGN-SA-HI
D
PBS
SA-PGN-Invivogen
BS-PGN-Invivogen
mTLR2 activity (OD 620)
10µg/mL
1µg/mL
0.1µg/mL

Figure S5

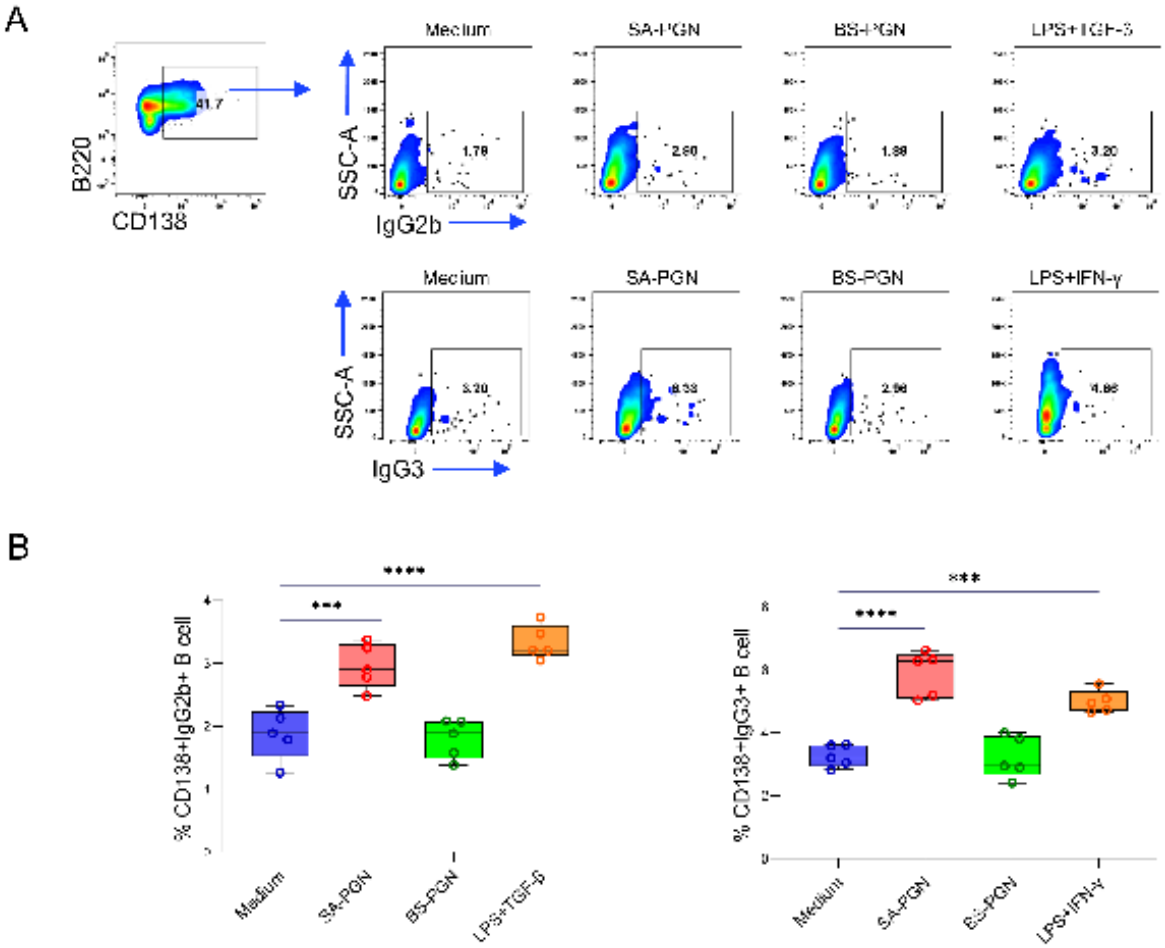
A
B220
CD138
41.7
SSC-A
IgG2b
Medium
SA-PGN
BS-PGN
LPS+TGF-β
1.78
2.60
1.88
3.20
IgG3
LPS+IFN-γ
3.20
8.33
2.98
4.86
B
% CD138+IgG2b+ B cell
% CD138−IgG3+ B cell
****
***
Medium
SA-PGN
BS-PGN
LPS+TGF-β
LPS+IFN-γ

Figure S6